Magnetic moment force and semi-free electrons: A unified analytical theory for anomalous transport in tokamak plasmas

Yuanjie Huang*

Mianyang, *Sichuan province*, *People's Republic of China*

*Corresponding author's E-mail: hyj201207@163.com

Abstract

The long-standing problem of anomalous transport in magnetic confinement plasmas, particularly in tokamaks, remains elusive despite many theoretical efforts such as the neoclassical theory. In this work, we present a fundamentally different analytical framework based on two previously overlooked physical insights into quasi-neutral plasma behavior under magnetic fields. First, we demonstrate that the conventional Lorentz force acting on charged particles, when averaged over a complete helical orbit, manifests as the magnetic moment force. Second, we propose that free electrons in a quasi-neutral plasma should be regarded as "semi-free", as their positional degrees of freedom are constrained by the ions within the framework of calculus due to charge neutrality. Based on these premises, a simple yet comprehensive analytical model is constructed. The model successfully reproduces the experimentally observed magnitudes of particle diffusion coefficients and thermal diffusivities, which are several orders higher than classical and neoclassical predictions. Furthermore, it provides a unified physical explanation for the formation of both the edge transport barrier (ETB) in H-mode and the internal transport barrier (ITB), linking them directly to temperature and pressure profile modifications. The derived radial electric field exhibits a negative

sign and the correct order of magnitude, consistent with experimental measurements, a feature not captured by classical treatments. These findings suggest that the so-called "anomalous" transport may be understood within a collision-dominated framework. The proposed model offers a new theoretical basis for understanding confinement degradation and improving operational performance in future fusion reactors.

Keywords：anomalous transport; magnetic confinement; tokamak plasma; diffusion constant; edge transport barrier; internal transport barrier

1. Introduction

Transport phenomena in magnetically confined plasmas have long been a central concern in magnetic confinement fusion research. Early theoretical efforts, based on a uniform magnetic field, gave rise to the classical theory of transport. However, the radial particle diffusion coefficients predicted by this classical framework were found to be several orders of magnitude lower than experimental measurements. In an attempt to resolve this discrepancy, the non-uniformity of magnetic field lines in toroidal geometry was incorporated, leading to the development of neoclassical transport theory [1, 2]. While neoclassical theory succeeded in increasing the predicted radial diffusion coefficient by one to two orders of magnitude [3], it still falls significantly short of explaining the experimentally observed values, which typically range from 1 to 10 m^2/s [3–9]. Moreover, experimental measurements have shown that radial thermal diffusivities for both ions and electrons are approximately two orders of magnitude larger than neoclassical predictions [4]. These discrepancies, observed across a wide range of experiments, have come to be known as anomalous transport [3, 4, 10, 11].

Over recent decades, substantial efforts have been devoted to addressing the anomalous transport problem. These include magnetohydrodynamic (MHD) models in axisymmetric toroidal geometry [12, 13], turbulent diffusion models based on micro-instabilities [11, 13, 14], and theories invoking large-scale collective motions [11, 15]. Despite these advances, constructing a comprehensive turbulence model remains extremely challenging due to the vast disparity between the spatial scales of turbulent structures and the markedly different timescales governing electron and ion motions [16, 17]. Consequently, a satisfactory analytical model capable of describing anomalous

transport in magnetically confined plasmas has remained elusive, representing a long-standing gap in plasma physics [3].

In this work, we propose a simple yet novel analytical model to describe the anomalous transport behavior of magnetically confined plasmas, with particular emphasis on tokamak configurations. The model is founded on two key physical insights into the behavior of quasi-neutral plasmas under magnetic fields, which challenge conventional assumptions and offer a fresh perspective on the underlying transport mechanisms.

The paper is organized as follows. Section 2 presents the theoretical framework and associated discussions. Within this section, Section 2.1 presents the two main physical insights for the analytical model. Section 3 presents the main results and discussion. In the sections, Section 3.1 develops the transport model for a cylindrical plasma column under a longitudinal magnetic field, serving as a foundational step. Section 3.2 then extends the model to the more complex geometry of a tokamak plasma. Section 3.3 discusses the assumptions and limitations of the model. Section 4 presents the comparison with the turbulence theory. Finally, Section 5 summarizes the main conclusions of this work.

2. Theory and Method

2.1 Two Fundamental Physical Insights

2.1.1 Semi-free electrons in neutral plasma

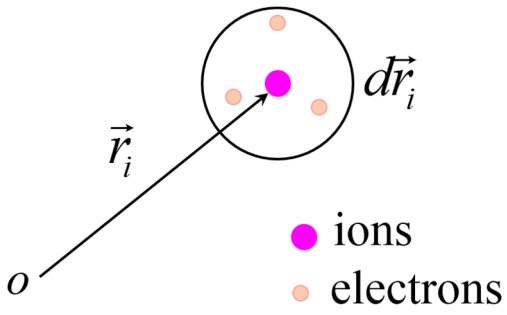

Figure 1 Schematic diagram for the quasi-neutral plasma with electrons (orange circles) and the ions (magenta circles) in the mathematical micro-element.

In a steady-state quasi-neutral plasma, the number of ions is approximately equal to that of electrons. Owing to charge neutrality, the positions of ions and electrons cannot be distinguished within an infinitesimal volume element in the sense of calculus. Moreover, the momentum of such a volume element is dominated by ions due to their much larger masses. Consequently, free electrons do not possess independent positional degrees of freedom and their positions are determined by the ions in the same volume element through the strong electrostatic force. This situation is analogous to that of neutral gases, in which light electrons are bound to heavy nuclei and thus lack positional degrees of freedom. Therefore, free electrons in a quasi-neutral plasma are more appropriately described as semi-free electrons. This concept constitutes a crucial physical insight for understanding transport phenomena in quasi-neutral plasmas. This concept, detailed in a separate work [18], is briefly summarized here for completeness.

Accordingly, the spatial gradient of the electron distribution function with

respect to electron position vanishes:

$$\nabla_{r_e} f_e = 0 \tag{1}$$

where r_e denotes the electron position and f_e is the distribution function for semi-free electrons. This treatment deviates substantially from conventional theoretical approaches and, as shown later, determines the sign of the radial electrostatic field along the minor radius in tokamak plasmas.

2.1.2 Magnetic moment force: gyro-averaged description of Lorentz force

In the presence of a magnetic field, a charged particle experiences the Lorentz force and typically follows a helical trajectory. According to conventional transport theory, the Lorentz force does no work, as it remains perpendicular to the particle velocity.

On time and spatial scales much larger than the gyroperiod and gyroradius, the particle motion can be described in terms of the motion of its guiding center. Over a complete gyroperiod, the guiding center experiences a net drift force resulting from the Lorentz force. Under the condition $|r_{Ac}\nabla B_z| \ll B_z$, this drift force reduces to the magnetic moment force [10],

$$\vec{F}_{mA} = -\frac{m_A v_{A\perp}^2}{2B_z}\nabla_\perp B_z \tag{2}$$

where the subscript $A = i, e$ denotes ions and electrons, r_{Ac} is the gyration radius, F_{mA} the magnetic moment force, $v_{A\perp}$ the particle velocity perpendicular to the magnetic field, and B_z the magnetic field strength along the z direction.

Thus, when averaged over complete gyroperiods, the Lorentz force effectively manifests as the magnetic moment force. Replacing the Lorentz force with this

averaged form has profound implications for charged particle transport, as will be shown in Section 3.2. This constitutes the second key physical insight underpinning the present study of magnetically confined plasmas.

3. Results and Discussion

For a high-temperature, low-density nondegenerate plasma, the Maxwell distribution is expected to be a valid description for both electrons and ions. The isotropic Maxwell distribution function can be written as $f_A^0 = n_A(\vec{r}_i,\ t)exp(-v_A^2/v_{AT}^2)/\pi^{3/2}v_{AT}^3$, where $n_A(r_i, t)$ is the number density dependent on the ion position r_i and time t, and $v_{AT} = \sqrt{2k_BT_A/m_A}$ is the thermal velocity with k_B the Boltzmann constant, m_A the particle mass, and T_A the spatially dependent temperature.

Following the Spitzer-Härm (SH) theory [19], the distribution function for each species can be expressed as the sum of an isotropic part and a small anisotropic perturbation $f_A = f_A^0 + f_A^1$, where f_A^1 denotes the anisotropic component. Within the framework of the non-equilibrium Boltzmann transport equation and the SH theory, the anisotropic component of the electron distribution function in the presence of an electric field and a magnetic field is given by $\left(e\vec{E}_r + F_{me}\right) \cdot \nabla_{v_e} f_e^0/m_e = -f_e^1/\tau_e$, where v_e is the electron velocity, e the elementary charge, E_r the electric field, and τ_e the electron relaxation time associated with electron–ion Coulomb collisions [19]. Substituting the Maxwell distribution f_A^0 into the above equation yields $f_e^1 = \tau_e\left(e\vec{E}_r + \vec{F}_{me}\right) \cdot \vec{v}_e f_e^0/k_BT_e$. The result plays a central role in the analysis of plasma

transport properties presented in the following sections.

3.1 Cylindrical plasma transport in a magnetic Field

3.1.1 Radial diffusion

A cylindrical plasma is considered in an externally applied magnetic field along the z-direction in cylindrical coordinates (r, θ, z). The plasma density and temperature gradients are assumed to be in the radial direction, leading to radial diffusion from the high-pressure core to the low-pressure edge. This radial diffusion can induce a poloidal electric field and an associated electric current via the electromotive force arising from the Lorentz force. The resulting poloidal electric current, in turn, weakens the magnetic field, which may vary slowly in the radial direction. Consequently, the plasma is subject to the electrostatic force, the magnetic moment force, and the inertial centrifugal force.

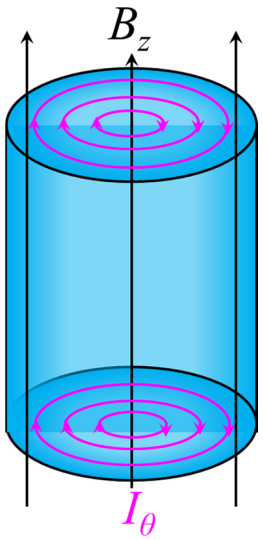

Figure 2. Schematic diagram of the cylindrical plasma under a magnetic field. The magnitude of the magnetic field (black arrows) may be partially canceled by the clockwise currents (magenta arrows) in the plasma.

Thus, the anisotropic components of the electron and ion distribution functions can be obtained.

$$f_e^1 = \frac{\tau_e f_e^0 \vec{v}_e \cdot}{k_B T_e}\left[e\vec{E}_r - \frac{m_e v_{e\perp}^2}{2B_z(r)}\nabla B_z(r) + \frac{m_e v_{e\theta}^2}{r^2}\vec{r} + e\vec{E}_\theta(r)\right]$$

$$f_i^1 = \frac{\tau_i f_i^0 \vec{v}_i \cdot}{k_B T_i}\left[-k_B T_i \nabla \ln p_i(r) - k_B T_i\left(\frac{v_i^2}{v_{iT}^2} - \frac{5}{2}\right)\nabla \ln T_i - Ze\vec{E}_r - \frac{m_i v_{i\perp}^2}{2B_z(r)}\nabla B_z(r) + \frac{m_i v_{i\theta}^2}{r^2}\vec{r} - Ze\vec{E}_\theta(r)\right]$$

where E_θ is the poloidal electric field in the plasma, τ_i signifies the ion relaxation time due to Coulomb collisions [19], and Z denotes the net charge number of the ion. The terms $m_i v_{i\theta}^2 \vec{r}/r^2$ and $m_e v_{e\theta}^2 \vec{r}/r^2$ represent the inertial centrifugal forces for the ions and electrons, respectively.

The electric current density can be expressed as $j_e = e\int d\vec{v}_e \vec{v}_e f_e^1 - Ze\int d\vec{v}_i \vec{v}_i f_i^1$ where j_e denotes the electric current. Following the mathematical formulation in Ref. [19], the radial electric current can be written as

$$j_{er} = en_e(\vec{r}_i)\left(\frac{\tau_e}{m_e} + \frac{Z\tau_i}{m_i}\right)e\vec{E}_r - en_e(\vec{r}_i)\left(\frac{\tau_e T_e}{m_e} - \frac{\tau_i T_i}{m_i}\right)\frac{5k_B}{3}\nabla \ln \frac{B_z(r)}{r} + en_e(\vec{r}_i)\frac{\tau_i}{m_i}k_B T_i \nabla \ln p_i(r)$$

where j_{er} denotes the radial electric current. Electrical transport processes typically occur on much faster timescales than thermal transport, justifying the assumption of charge neutrality, which requires the radial electric current to vanish. This assumption, widely adopted in related theoretical studies, enables the determination of the electric field E_0

$$e\vec{E}_r = -\frac{\tau_i}{m_i}\left(\frac{\tau_e}{m_e} + \frac{Z\tau_i}{m_i}\right)^{-1} k_B T_i \nabla_{\vec{r}} \ln p_i(r) + \left(\frac{\tau_e T_e}{m_e} - \frac{\tau_i T_i}{m_i}\right)\left(\frac{\tau_e}{m_e} + \frac{Z\tau_i}{m_i}\right)^{-1}\frac{5k_B}{3}\nabla \ln \frac{B_z(r)}{r} \quad (3)$$

It follows that the electrons and ions share the same mean radial velocity,

$$u_r = -\frac{\tau_e}{m_e}\frac{\tau_i}{m_i}\left(\frac{\tau_e}{m_e}+\frac{Z\tau_i}{m_i}\right)^{-1}\left[k_B T_i \nabla \ln p_i(r) + \frac{5k_B(ZT_e+T_i)}{3}\nabla \ln \frac{B_z(r)}{r}\right] \tag{4}$$

Once the position-dependent magnetic field is determined, the radial velocity of the plasma can be obtained.

Based on Maxwell equations, the magnetic field depends on the poloidal electric current as follows $\partial B_z(r)/\partial r = -\mu_0 \sigma_e E_\theta$, where μ_0 denotes the vacuum permeability, and σ_e is the electrical conductivity. The poloidal electric field E_θ arises from the time-varying enclosed magnetic flux and can be expressed as $E_\theta = -u_r B_z(r) - r^{-1}\int_0^r r' dr' \, \partial B_z(r')/\partial t$. When the plasma is in a steady state, the magnetic field does not vary significantly with time, leading to the relation $E_\theta \approx -u_r B_z(r)$. Therefore, the relation between the magnetic field and the radial velocity can be obtained as

$$\frac{\partial}{\partial r}\ln B_z(r) = \mu_0 \sigma_e u_r \tag{5}$$

Substituting Eq. (5) into Eq. (4) yields

$$u_r = \frac{\frac{\tau_e}{m_e}\frac{\tau_i}{m_i}\left(\frac{\tau_e}{m_e}+\frac{Z\tau_i}{m_i}\right)^{-1}\left[-k_B T_i \frac{\partial}{\partial r}\ln p_i(r) + \frac{5k_B(ZT_e+T_i)}{3r}\right]}{1+\frac{\tau_e}{m_e}\frac{\tau_i}{m_i}\left(\frac{\tau_e}{m_e}+\frac{Z\tau_i}{m_i}\right)^{-1}\frac{5k_B(ZT_e+T_i)}{3}\mu_0\sigma_e} \tag{6}$$

In general, the temperature of a tokamak plasma is much higher than 10^5 *K*. Consequently, the second term in the denominator of the above equation is significantly larger than unity, allowing the approximation

$$u_r \approx \frac{1}{\mu_0\sigma_e}\left[-\frac{3}{5}\frac{T_i}{(ZT_e+T_i)}\frac{\partial}{\partial r}\ln p_i(r) + \frac{1}{r}\right] \tag{7}$$

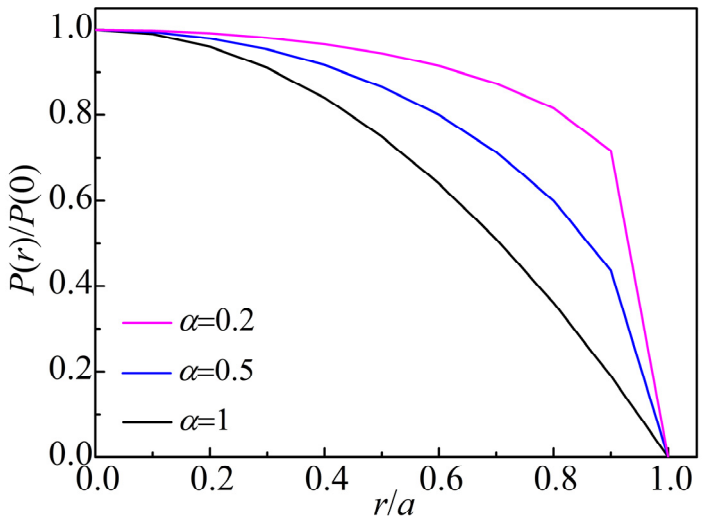

Figure 3. The reduced plasma pressure versus the reduced minor radius. The lines are given by the function $p_i(r)/p_i(0) = (1 - r^2/a^2)^{\alpha}$, α=1 for the black line, α=0.5 for the blue line and α=0.2 for the magenta line.

From Eq. (5) and Eq. (7), the condition $|r_{Ac}\nabla B_z| \ll B_z$ is often satisfied, confirming that Eq. (2) is applicable to the plasma.

The mean radial velocity exhibits several important properties.

First, the radial velocity depends strongly on the temperature and scales as $u_r \propto T_e^{-1.5}$, since the electron relaxation time obeys $\tau_e \propto T_e^{1.5}$ according to Coulomb collisions [19].

Second, the mean radial velocity is proportional to the net charge number Z of the ion, and the ions with a higher net charge lead to a larger radial velocity. This is because a higher ion charge significantly reduces the electron relaxation time via Coulomb collisions [19].

Third, the radial velocity at the plasma edge can be influenced by the pressure gradient. In many tokamak plasmas, the plasma pressure is commonly described by

$p_i(r)/p_i(0) = (1 - r^2/a^2)^{\alpha}$ [20], [21]. When the plasma pressure exhibits a pedestal at the edge, corresponding to a small value of the index α, as shown in Figure 3, the radial velocity becomes small. Raising the temperature at the plasma edge is expected to reduce the radial velocity and improve the confinement performance, which is consistent with the experimental observations of H-mode tokamak plasma [22], [23]. Therefore, both the pressure pedestal and the elevated edge temperature contribute to a reduction in the mean radial velocity, which may underlie the formation of the edge transport barrier (ETB).

Fourth, the radial velocity near the plasma core is dominated by the second term arising from the inertial centrifugal forces. The plasma close to the core may exhibit a notable radial velocity, which can help prevent the plasma accumulation. However, an elevated temperature is expected to significantly reduce both the radial velocity and the associated diffusivity at the core region, which agrees with the experimental observations [24], [25]. A steep pressure gradient at the tokamak core corresponds to a small value of the index β when the plasma pressure is described by $p_i(r)/p_i(0) = (1 - r^2/r_I^2)^{\beta}$, where β is a dimensionless index, r_I denotes the location of internal transport barrier (ITB). Both a small β and an increased temperature near the core can reduce the radial velocity, suggesting a possible mechanism for the formation of ITB. It is worth noting that while the formation of ITB and ETB indeed reduces the radial velocity, the reduction factor is typically several times at most, but hardly reaches an order of magnitude, which is consistent with experimental results [22]. Both the ETB and ITB may share the same underlying physical mechanism, implying that a third steep

pressure gradient could similarly improve confinement performance.

Fifth, the magnitude of the radial velocity and the associated diffusion coefficient at the plasma edge can be estimated using typical parameters, as shown in Figure 4. The radial velocity obtained in the work is several orders of magnitude higher than that predicted by the classical theory.

Sixth, the magnetic moment force, rather than the Lorentz force, is responsible for the plasma confinement. This observation suggests that the magnetic field may enter the well-known Fokker-Planck equation in the form of the magnetic moment force rather than the Lorentz force, a point that differs significantly from the case of a single charged particle in a magnetic field. Although the radial velocity is clearly confined by the external magnetic field, its mathematical expression does not explicitly contain the magnetic field.

When the plasma reaches thermal equilibrium, the electron and ion temperatures become equal. The relevant diffusion constant can be expressed as

$$D_r = \frac{1}{\mu_0 \sigma_e}\left[\frac{3}{5(Z+1)}\left(1+\frac{\partial \ln T}{\partial \ln n_i}\right)-\left(\frac{\partial \ln n_i}{\partial \ln r}\right)^{-1}\right] \tag{8}$$

where D_r denotes radial diffusion constant. The magnitude of the diffusion constant can be estimated under typical conditions. For the plasma edge with parameters $\partial lnT/\partial lnn_i = 4$, $\partial lnn_i/\partial lnr = -10$, and Z=1, the temperature-dependent diffusion constant is shown in Figure 4. The radial diffusion constant obtained in the work is several orders of magnitude larger than that predicted by classical theory. At the plasma edge with a temperature of 10^6 K, the radial diffusion constant is approximately 5 m^2/s, a value whose order of magnitude is consistent with

the experimental findings [3]–[8]. Furthermore, as the plasma temperature increases toward the core, the radial diffusion constant gradually decreases. This trend agrees with the experimental results showing a reduction in the radial diffusion constant near the plasma core [3], [4], [7].

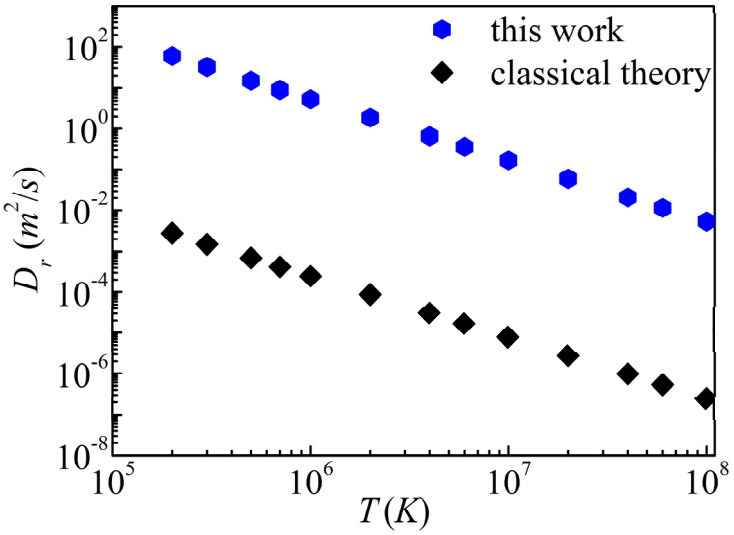

Figure 4. Temperature dependence of the radial diffusion constant for the plasma edge in cylindrical coordinates.

Moreover, the ratio of the diffusion constant obtained in this study to that from classical theory can be given by

$$\frac{D_r}{D_{cr}} \approx \frac{3}{5(Z+1)} \frac{B_z^2(r)}{\mu_0 p_i(r)} \tag{9}$$

where D_{cr} denotes the radial diffusion constant based on classical theory. As shown, this ratio can reach 10^4 for an ion pressure 10^2 *Pa* at the tokamak plasma edge under an externally magnetic field of 3 *T*.

Through straightforward calculations, the position-dependent magnetic field can be formulated as

$$B_z(r) = B_z(a)\frac{r}{a}\left[\frac{p_i(a)}{p_i(r)}\right]^{\frac{3}{5(Z+1)}} \tag{10}$$

where $B_z(a)$ denotes the externally applied magnetic field and a is the plasma radius. It indicates that the magnetic field continuously decreases toward the plasma core due to the poloidal current. Moreover, a large pressure corresponds to a small magnetic field in a steady-state plasma.

3.1.2 Radial thermal conductivity

The mathematical expression for the mean radial velocity in Eq. (6) suggests that the radial mobility of the electrons and ions can be given by

$$\frac{\tau_{im}}{m_i} = \frac{\tau_{em}}{m_e} = \frac{\frac{\tau_e}{m_e}\frac{\tau_i}{m_i}\left(\frac{\tau_e}{m_e}+\frac{Z\tau_i}{m_i}\right)^{-1}}{1+\frac{\tau_e}{m_e}\frac{\tau_i}{m_i}\left(\frac{\tau_e}{m_e}+\frac{Z\tau_i}{m_i}\right)^{-1}\frac{5(Z+1)k_BT_e}{3}\mu_0\sigma_e} \tag{11}$$

where τ_{em} and τ_{im} denote the modified relaxation times in the radial direction for the electron and ions under the magnetic field, respectively.

The radial electron and ion heat fluxes are given by $j_{eqr} = \int d\vec{v}_e f_e^1 \vec{v}_e \, m_e v_e^2/2$ and $j_{iqr} = \int d\vec{v}_i f_i^1 \vec{v}_i \, m_i v_i^2/2$, where j_{eqr} and j_{iqr} denote the radial electron heat flux and radial ion heat flux, respectively. Through simple calculations, the heat fluxes can be written as

$$j_{eqr} = \frac{5n_e}{2}\left(k_BT_e\right)^2\frac{\tau_{em}}{m_e}\left[-\frac{T_i}{T_e}\nabla_{\vec{r}}\ln p_i + \frac{7}{3r}\right] \tag{12}$$

$$j_{iqr} = \frac{5}{2}n_i\left(k_BT_i\right)^2\frac{\tau_{im}}{m_i}\left[-\nabla_{\vec{r}}\ln p_i(\vec{r}) - \nabla_{\vec{r}}\ln T_i + \frac{7}{3r}\right] \tag{13}$$

Therefore, the electron and ion thermal conductivity in the radial direction can be obtained as

$$\kappa_{er}=\frac{3n_ek_B}{2(Z+1)\mu_0\sigma_e(r)}\left[\left(1+\frac{\partial\ln n_i}{\partial\ln T_i}\right)\frac{\partial T_i}{\partial T_e}-\frac{7}{3}\left(\frac{\partial\ln T_e}{\partial\ln r}\right)^{-1}\right] \tag{14}$$

$$\kappa_{ir}=\frac{3n_ik_B}{2(Z+1)\mu_0\sigma_e(r)}\frac{T_i}{T_e}\left[2+\frac{\partial\ln n_i}{\partial\ln T_i}-\frac{7}{3}\left(\frac{\partial\ln T_i}{\partial\ln r}\right)^{-1}\right] \tag{15}$$

where κ_{er} and κ_{ir} represent the radial thermal conductivities for the electrons and ions, respectively. As shown, the electron radial thermal conductivity is comparable in magnitude to the ion radial thermal conductivity, which is consistent with the experimental observations [4], [6], [26]. The total thermal conductivity of the plasma can then be written as

$$\kappa=\frac{3n_ik_B}{2(Z+1)\mu_0\sigma_e(r)}\left[Z\left(1+\frac{\partial\ln n_i}{\partial\ln T_i}\right)\frac{\partial T_i}{\partial T_e}-\frac{7Z}{3}\left(\frac{\partial\ln T_e}{\partial\ln r}\right)^{-1}+\frac{T_i}{T_e}\left(2+\frac{\partial\ln n_i}{\partial\ln T_i}\right)-\frac{T_i}{T_e}\frac{7}{3}\left(\frac{\partial\ln T_i}{\partial\ln r}\right)^{-1}\right]$$

In the case of the thermal equilibrium, *i.e.*, T_e=T_i, the thermal conductivity can be simplified to

$$\kappa=\frac{3n_ik_B}{2\mu_0\sigma_e(r)}\left[\frac{Z+2}{Z+1}+\frac{\partial\ln n_i}{\partial\ln T_i}-\frac{7}{3}\left(\frac{\partial\ln T}{\partial\ln r}\right)^{-1}\right] \tag{16}$$

The related thermal diffusivities can be expressed as

$$\chi_{er}=\frac{1}{(Z+1)\mu_0\sigma_e(r)}\left[\left(1+\frac{\partial\ln n_i}{\partial\ln T_i}\right)\frac{\partial T_i}{\partial T_e}-\frac{7}{3}\left(\frac{\partial\ln T_e}{\partial\ln r}\right)^{-1}\right] \tag{17}$$

$$\chi_{ir}=\frac{1}{(Z+1)\mu_0\sigma_e(r)}\frac{T_i}{T_e}\left[2+\frac{\partial\ln n_i}{\partial\ln T_i}-\frac{7}{3}\left(\frac{\partial\ln T_i}{\partial\ln r}\right)^{-1}\right] \tag{18}$$

where χ_{er} and χ_{ir} denote the radial thermal diffusivities for the electrons and ions, respectively. These expressions indicate that the thermal diffusivities are mathematically independent of both the magnetic field and the particle density, a result consistent with the experimental findings [27]. Furthermore, an increase in the plasma core temperature leads to a reduction in the thermal diffusivity, which also agrees with the experimental results [24].

According to the classical theory, the radial thermal conductivity can be written as

$$\kappa_c = \frac{5(Z+1)n_i k_B}{4\mu_0\sigma_e}\frac{p_i}{B_z^2(r)/2\mu_0}\left[\frac{Z+2}{Z+1}+\frac{\partial \ln n_i}{\partial \ln T}-\frac{7}{3}\left(\frac{\partial \ln T}{\partial \ln r}\right)^{-1}\right]$$

where κ_c denotes the radial thermal conductivity based on the classical theory. The ratio of the thermal conductivity obtained in the work to the classical value is given by

$$\frac{\kappa}{\kappa_c} = \frac{3}{5(Z+1)}\frac{B_z^2(r)}{\mu_0 p_i} \tag{19}$$

Substituting Eq. (10) into the above equation yields

$$\frac{\kappa}{\kappa_c} = \frac{3}{5(Z+1)}\frac{B_z^2(a)}{\mu_0 p_i(a)}\frac{r^2}{a^2}\left[\frac{p_i(a)}{p_i(r)}\right]^{1+\frac{6}{5(Z+1)}} \tag{20}$$

This indicates that the ratio decreases continuously with decreasing radius. At the tokamak plasma edge with the typical parameters of an ion pressure of 10^2 *Pa* and a magnetic field of 3 *T*, the thermal conductivity ratio reaches 10^4, demonstrating that the thermal conductivity in the work is significantly larger than that predicted by the classical theory. Interestingly, a comparison between the ratio of the diffusion constants in Eq. (9) and the ratio of thermal conductivities in Eq. (19) reveals that the two ratios are identical. The theoretical treatments of the cylindrical plasma presented here may provide insights for understanding the underlying physics of the tokamak plasmas.

3.2 The anomalous transport of tokamak plasma

3.2.1 Radial diffusion

For a tokamak plasma, the coordinate system (r, θ, φ) is commonly employed. In the framework, the magnetic field can be expressed in terms of its θ and φ components.

The Maxwell equations governing the magnetic field can be written as

$$\mu_0\left(\sigma_e E_\theta \vec{e}_\theta + \sigma_e E_\varphi \vec{e}_\varphi\right) = \frac{1}{r\left(R + r\cos\theta\right)}\left\{\vec{e}_r\left[\frac{\partial}{\partial\theta}\left(R + r\cos\theta\right)B_\varphi - \frac{\partial}{\partial\varphi}rB_\theta\right] - r\vec{e}_\theta\frac{\partial}{\partial r}\left(R + r\cos\theta\right)B_\varphi + \left(R + r\cos\theta\right)\vec{e}_\varphi\frac{\partial}{\partial r}rB_\theta\right\}$$

$$0 = \frac{1}{r\left(R + r\cos\theta\right)}\left[\frac{\partial}{\partial\theta}\left(R + r\cos\theta\right)B_\theta + \frac{\partial}{\partial\varphi}rB_\varphi\right]$$

where E_φ denotes the electric field in the φ direction, and R is the major radius. Owing to the axisymmetry, the magnetic field is independent of the toroidal angle φ, which leads to the following relations

$$\mu_0\sigma_e E_\varphi = \frac{1}{r}\frac{\partial}{\partial r}rB_\theta\left(r\right)$$

$$\mu_0\sigma_e E_\theta = -\frac{1}{\left(R + r\cos\theta\right)}\frac{\partial}{\partial r}\left(R + r\cos\theta\right)B_\varphi\left(r\right)$$

As previously established, the poloidal electric field in a steady-state plasma is given by $E_\theta = -u_r B_\varphi(r)$. Substituting this expression into the above equations yields

$$\mu_0\sigma_e u_r = \frac{\partial}{\partial r}\ln\left[\left(R + r\cos\theta\right)B_\varphi\left(r\right)\right] \tag{21}$$

On the other hand, the toroidal electric field consists of two contributions: the magnetically induced electric field and the self-induced field arising from the Lorentz force,

$$\mu_0\sigma_e\left[E_{in} + u_r B_\theta\left(r\right)\right] = \frac{1}{r}\frac{\partial}{\partial r}rB_\theta\left(r\right) \tag{22}$$

where E_{in} represents the magnetically induced toroidal electric field, and the second term originates from the Lorentz force.

The average Lorentz force acting on the charged particles over the gyroperiods must be considered. The theoretical treatment follows that in Ref. [10]. The dynamic equation for a charged particle in a uniform plasma can be written as $m\,\partial v_r/\partial t = q\left(v_\theta B_\varphi - v_\varphi B_\theta\right)$, where *m and q* signifies the mass and the charge of the particle,

respectively, v_θ denotes the poloidal velocity, and v_φ the toroidal velocity. A complete period of the particle motion consists of k poloidal periods and l toroidal periods, during which the average radial velocity vanishes [10].

$$0 = q\left[B_\varphi(r)(\theta_2 - \theta_1) + \frac{\partial B_\varphi(r)}{\partial r} k\pi r_\theta^2 \right] - q\left[(R + r\cos\theta) B_\theta(r)(\varphi_2 - \varphi_1) - \frac{\partial B_\theta(r)}{\partial r} l\pi r_\varphi^2 \right]$$

where r_θ and r_φ represent the radius of the helical motion in the poloidal and toroidal directions, respectively, k and l are the integer numbers. Dividing the complete period yields

$$0 = qB_\varphi(r)u_\theta + q\frac{\partial B_\varphi(r)}{\partial r}\frac{k\pi r_\theta^2 \omega_\theta}{k2\pi} - \left[q(R + r\cos\theta) B_\theta(r) u_\varphi - q\frac{\partial B_\theta(r)}{\partial r}\frac{l\pi r_\varphi^2 \omega_\varphi}{k2\pi} \right]$$

where u_θ, u_φ denotes the average poloidal and toroidal velocities, respectively, ω_θ and ω_φ are the corresponding poloidal and the toroidal angular velocities. These quantities are given by $r_\theta = m\sqrt{v_r^2 + v_\theta^2}/qB_\varphi(r)$, $\omega_\theta = qB_\varphi(r)/m$, $r_\varphi = m\sqrt{v_r^2 + v_\varphi^2}/qB_\theta(r)$, $\omega_\varphi = qB_\theta(r)/m$. Substituting these expressions into the above equation leads to

$$qu_\theta B_\varphi(r) - qu_\varphi B_\theta(r) = -\frac{m\left(v_r^2 + v_\theta^2\right)}{2B_\varphi(r)}\frac{\partial B_\varphi(r)}{\partial r} - \frac{m\left(v_r^2 + v_\varphi^2\right)}{2B_\theta(r)}\frac{\partial B_\theta(r)}{\partial r} \qquad (23)$$

Over a complete period, the Lorentz force on a charged particle reduces to a mathematical form analogous to magnetic moment force. This equivalence is a key insight of the present work. Consequently, the mean radial electron velocity can be derived as

$$u_{er} = \frac{\tau_e}{m_e} eE_r - \frac{\tau_e}{m_e}\frac{5k_B T_e}{3}\frac{\partial \ln B_\varphi(r) B_\theta(r)}{\partial r} + \frac{\tau_e}{m_e}\frac{5k_B T_e}{3}\frac{\partial \ln r(R + r\cos\theta)}{\partial r} \qquad (24)$$

where E'_0 denotes the electrostatic field in the radial direction. The mean radial ion

velocity can be obtained in a similar manner

$$u_{ir} = -\frac{\tau_i}{m_i} k_B T_i \nabla_{\vec{r}} \ln p_i(r) - \frac{\tau_i}{m_i} ZeE_r - \frac{\tau_i}{m_i} \frac{5k_B T_i}{3} \frac{\partial}{\partial r} \ln \frac{B_\varphi(r) B_\theta(r)}{r(R + r\cos\theta)} \tag{25}$$

The neutrality condition requires that the mean radial electron velocity be equal to the mean radial ion velocity, which yields

$$u_r = \frac{-\frac{\tau_e}{m_e}\frac{\tau_i}{m_i} k_B T_i \nabla_{\vec{r}} \ln p_i(r) - \frac{\tau_e}{m_e}\frac{\tau_i}{m_i} \frac{5k_B(ZT_e + T_i)}{3} \left[\frac{\mu_0 \sigma_e E_{in}}{B_\theta(r)} - \frac{R + 2r\cos\theta}{r(R + r\cos\theta)} \right]}{\left(\frac{\tau_e}{m_e} + \frac{Z\tau_i}{m_i} \right) \left[1 + \frac{\tau_e}{m_e}\frac{\tau_i}{m_i} \left(\frac{\tau_e}{m_e} + \frac{Z\tau_i}{m_i} \right)^{-1} \frac{10k_B(ZT_e + T_i)}{3} \mu_0 \sigma_e \right]} \tag{26}$$

where u_r denotes the mean radial velocity for both ions and electrons. For a tokamak plasma, the following condition generally holds

$$\frac{\tau_e}{m_e}\frac{\tau_i}{m_i} \left(\frac{\tau_e}{m_e} + \frac{Z\tau_i}{m_i} \right)^{-1} \frac{10k_B(ZT_e + T_i)}{3} \mu_0 \sigma_e >> 1$$

Thus, the mean radial velocity can be approximated as

$$u_r \approx \frac{1}{\mu_0 \sigma_e} \left[-\frac{3}{10} \frac{T_i}{(ZT_e + T_i)} \frac{\partial}{\partial r} \ln p_i(r) - \frac{\mu_0 \sigma_e E_{in}}{2B_\theta(r)} + \frac{1}{r} + \frac{\cos\theta}{(R + r\cos\theta)} \right] \tag{27}$$

and the radial electric field as

$$ZeE_r \approx -k_B T_i \nabla_{\vec{r}} \ln p_i(r) - \frac{5k_B T_i}{3} \frac{\partial \ln B_\varphi(r) B_\theta(r)}{\partial r} + \frac{5k_B T_i}{3} \frac{\partial \ln r(R + r\cos\theta)}{\partial r} \tag{28}$$

In the plasma core, the poloidal field may be expressed as $B_\theta(r) = Cr$, where C is a constant. Substituting this expression along with Eq. (27) into Eq. (22) yields

$$C \approx \frac{\mu_0 \sigma_e E_{in}}{2}$$

Finally, the mean radial velocity near the plasma core is obtained

$$u_r(r) \approx \frac{1}{\mu_0 \sigma_e} \left[-\frac{3}{10} \frac{T_i}{(ZT_e + T_i)} \frac{\partial}{\partial r} \ln p_i(r) + \frac{\cos\theta}{(R + r\cos\theta)} \right] \tag{29}$$

As shown, the toroidal electric current can significantly reduce the mean radial velocity

through the induced poloidal magnetic field. Specifically, the magnetically induced electric current density $\sigma_e E_{in}$ suppresses the radial velocity component driven by the inertial centrifugal force. Hence, an appropriate magnitude of $\sigma_e E_{in}$ is essential for achieving the effective confinement in a tokamak plasma. In addition, the spontaneous bootstrap current density $\sigma_e u_r B_\theta$ reduces by half the mean radial velocity component originating from the ion pressure gradient. The mean radial velocity can also be lowered by increasing the electron-to-ion temperature ratio.

The associated diffusion constant can be expressed as

$$D_r = \frac{1}{\mu_0 \sigma_e}\left[\frac{3}{10}\frac{T_i}{\left(ZT_e + T_i\right)}\left(1+\frac{\partial \ln T_i}{\partial \ln n_i}\right) - \frac{\cos\theta}{\left(R + r\cos\theta\right)}\left(\frac{\partial \ln n_i}{\partial r}\right)^{-1}\right] \tag{30}$$

If the tokamak plasma reaches the thermal equilibrium, the diffusion constant simplifies to

$$D_r = \frac{1}{\mu_0 \sigma_e}\left[\frac{3}{10\left(Z+1\right)}\left(1+\frac{\partial \ln T_i}{\partial \ln n_i}\right) - \frac{\cos\theta}{\left(R + r\cos\theta\right)}\left(\frac{\partial \ln n_i}{\partial r}\right)^{-1}\right] \tag{31}$$

It suggests that the radial diffusion constant can be significantly reduced by the poloidal magnetic field induced by the toroidal current. Furthermore, the poloidal field component arising from the bootstrap current reduces by half the diffusion term associated with the ion pressure gradient, while the poloidal field component due to the magnetically induced electric current cancels the diffusion term originating from the inertial centrifugal force along the minor radius r. This indicates that the diffusion in the plasma core is primarily suppressed by the poloidal field component driven by the magnetically induced electric current.

Based on the analytical expression, the magnitude of the diffusion constant can be

estimated. For the edge region of a tokamak plasma with the typical parameters $\partial lnT/\partial lnn_i = 4$, $\partial lnn_i/\partial lnr = -10$, Z=1, a/R=1/3, T=10^6 K, the radial diffusion constant is found to be approximately 2.6 m^2/s, in agreement with the order of magnitude reported in experimental studies [3], [5]–[8], [28], [29]. The radial diffusion constant is observed to decrease toward the plasma core with increasing the temperature, which is consistent with the experimental observations [3], [5], [7], [28], [29]. Given that the confinement time is inversely proportional to the radial diffusion constant [3], the plasma confinement time is anticipated to scale as $T^{3/2}$, in agreement with the experimental findings [30], [31].

As in the case of a cylindrical plasma described previously, although the radial diffusion constant is substantially reduced by the toroidal and the poloidal magnetic fields, it does not explicitly depend on the magnetic field strengths in its mathematical form. Consequently, the confinement time is inferred to be largely independent of the magnetic field and proportional to the electrical conductivity. This behavior is supported by the experimental scaling law$\tau \propto B_T^{0.15} I_P^{0.93}$ [32], where I_p denotes the toroidal current and B_T the toroidal magnetic field. The weak dependence on the toroidal field is likely attributable to the field dependence of the temperature, which will be addressed in the next section. Moreover, given that the electrical conductivity is independent of the plasma density under the Coulomb collision mechanism, the radial diffusion constant appears insensitive to the plasma density, a trend consistent with the experimental results [8].

Furthermore, the relationship between the ion pressure and the magnetic field

strength can be derived for a tokamak plasma in thermal equilibrium,

$$B_\varphi(r,\theta)B_\theta(r,\theta) = B_\varphi(a,\theta)B_\theta(a,\theta)\frac{r}{r_0}\frac{(R+r\cos\theta)}{(R+a\cos\theta)}\left[\frac{p_i(a,\theta)}{p_i(r,\theta)}\right]^{\frac{3}{5(Z+1)}} \tag{32}$$

Substituting the above equation into Eq. (28) yields

$$E_r = -\frac{k_B T_i}{(Z+1)e}\frac{\partial \ln p_i(r,\theta)}{\partial r} \tag{33}$$

It indicates that the radial electric field is negative, implying that it points toward the plasma core, a finding consistent with the experimental measurements [22], [33], [34]. In contrast, the sign of the radial electric field predicted by the classical theory is positive. The negative sign arises from the fact that the semi-free electrons lack the position degrees of freedom. When accounting for the position-dependent temperature and pressure, the radial electric field reaches values on the order of 10^4 *V/m* at the plasma edge, in agreement with the experimental observations [22], [33], [34]. Moreover, the radial electric field can be expressed using the generalized parabolic functions [14], [21] for the ion density and temperature profiles $n_i(r) = n_i(0)(1 - r^2/a^2)^{\alpha_n}$, $T_i(r) = T_i(0)(1 - r^2/a^2)^{\alpha_T}$, where $n_i(0)$ and $T_i(0)$ denote the ion density and temperature at the plasma core, respectively, α_n and α_T are the dimensionless exponents.

$$E_r = \frac{2k_B T_i(0)(\alpha_n + \alpha_T)}{(Z+1)e}\frac{r}{a^2}\left(1-\frac{r^2}{a^2}\right)^{\alpha_T - 1} \tag{34}$$

As the tokamak plasma enters the H-mode, the exponent α_T may decrease significantly, leading to an enhancement of the radial electrostatic field near the plasma edge, which is shown in Fig. 5, a behavior consistent with the experimental measurements [34]. Therefore, the enhanced magnitude of the negative radial electric field at the plasma

edge is the result rather than the source of the H-mode.

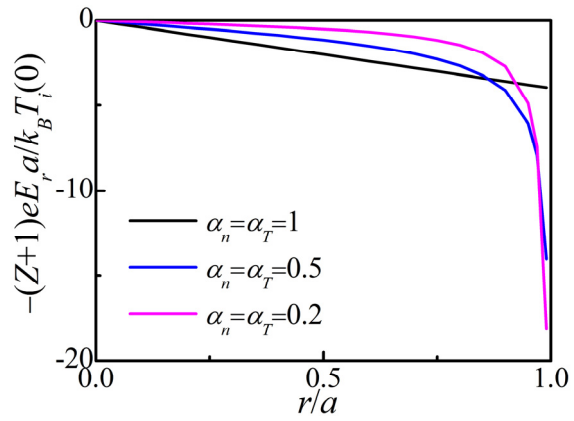

Figure 5. Reduced minor radius dependence of the reduced radial electric field. a denotes the minor radius, e the electron charge, E_r the radial electric field, k_B the Boltzmann constant, α_n and α_T are the dimensionless exponents in the ion density and temperature profiles $n_i(r) = n_i(0)(1 - r^2/a^2)^{\alpha_n}$, $T_i(r) = T_i(0)(1 - r^2/a^2)^{\alpha_T}$, where $n_i(0)$ and $T_i(0)$ denote the ion density and temperature at the plasma core, respectively.

Inserting Eq. (29) into Eq. (21) yields

$$\frac{\partial}{\partial r}\ln B_\varphi(r,\theta)+\frac{3}{10(Z+1)}\frac{\partial}{\partial r}\ln p_i(r,\theta)=0$$

Consequently, the spatial dependence of the toroidal magnetic field can be expressed as

$$B_\varphi(r,\theta)=B_\varphi(a,\theta)\left[\frac{p_i(a,\theta)}{p_i(r,\theta)}\right]^{\frac{3}{10(Z+1)}} \tag{35}$$

Substituting the position-dependent toroidal field into Eq. (32) gives

$$B_\theta(r,\theta)=B_\theta(a,\theta)\frac{r}{r_0}\frac{(R+r\cos\theta)}{(R+a\cos\theta)}\left[\frac{p_i(a,\theta)}{p_i(r,\theta)}\right]^{\frac{3}{10(Z+1)}} \tag{36}$$

In analogy with the treatment of the radial velocities, the poloidal velocities of the electrons and ions can be expressed as

$$u_{e\theta}=\frac{\tau_e}{m_e}\left[eE_\theta-\frac{5k_BT_e}{3}\frac{\partial\ln B_\varphi(r,\theta)}{r\partial\theta}-\frac{5k_BT_e}{3}\frac{\partial\ln B_\theta(r,\theta)}{r\partial\theta}-\frac{5k_BT_e\sin\theta}{3(R+r\cos\theta)}\right]$$

$$u_{i\theta}=\frac{\tau_i}{m_i}\left[-k_BT_i(\vec{r})\frac{\partial}{r\partial\theta}\ln p_i(r,\theta)-ZeE_\theta-\frac{5k_BT_i}{3}\frac{\partial\ln B_\varphi(r,\theta)B_\theta(r,\theta)}{r\partial\theta}-\frac{5k_BT_i\sin\theta}{3(R+r\cos\theta)}\right]$$

where E_θ denotes the poloidal electrostatic field. Under the steady-state conditions, the above poloidal velocities are equal to each other

$$0=-k_BT_i(\vec{r})\frac{\partial\ln p_i(r,\theta)}{r\partial\theta}-\frac{5k_B(ZT_e+T_i)}{3}\left[\frac{\partial\ln B_\varphi B_\theta(r,\theta)}{r\partial\theta}+\frac{\sin\theta}{(R+r\cos\theta)}\right] \quad (37)$$

If the electron temperature equals the ion temperature, the following relation is obtained

$$B_\varphi(r,\theta)B_\theta(r,\theta)=B_\varphi\left(r,\frac{\pi}{2}\right)B_\theta\left(r,\frac{\pi}{2}\right)\frac{(R+r\cos\theta)}{R}\left[\frac{p_i\left(r,\frac{\pi}{2}\right)}{p_i(r,\theta)}\right]^{\frac{3}{5(Z+1)}} \quad (38)$$

The Eq. (35), (36) and (37) collectively determine the dependence of the magnetic fields on both the radial position and poloidal angle.

3.2.2 Radial thermal conductivity

Due to the confinement provided by the toroidal and poloidal magnetic fields, the radial relaxation times for the electrons and ions in thermal equilibrium are modified as follows $\tau_{em}/m_e=\tau_{im}/m_i\approx 3/10(Z+1)\,k_BT\mu_0\sigma_e(r)$, where τ_{im} and τ_{em} denote the modified radial relaxation times for electrons and ions, respectively. Thereby the thermal conductivity of the tokamak plasma can be evaluated. Due to the plasma conservation, the radial heat fluxes contributed by the electrons and ions are given by

$$j_{eqr}=\frac{5}{2}n_e(k_BT)^2\frac{\tau_{em}}{m_e}\left[-\nabla_{\vec{r}}\ln p_i+\frac{7}{3}\frac{\cos\theta}{(R+r\cos\theta)}\right] \quad (39)$$

$$j_{iqr}=\frac{5}{2}n_i(k_BT)^2\frac{\tau_{im}}{m_i}\left[-\nabla_{\vec{r}}\ln p_i(\vec{r})-\nabla_{\vec{r}}\ln T+\frac{7}{3}\frac{\cos\theta}{(R+r\cos\theta)}\right] \quad (40)$$

where j_{eqr} and j_{iqr} represent the radial heat fluxes of the electrons and ions, respectively. The corresponding radial thermal conductivities are then expressed as

$$\kappa_{er}=\frac{3n_e k_B}{4(Z+1)\mu_0\sigma_e(r)}\left[1+\frac{\partial\ln n_i}{\partial\ln T}-\frac{7}{3}\left(\frac{\partial\ln T}{\partial r}\right)^{-1}\frac{\cos\theta}{(R+r\cos\theta)}\right] \tag{41}$$

$$\kappa_{ir}=\frac{3n_i k_B}{4(Z+1)\mu_0\sigma_e(r)}\left[2+\frac{\partial\ln n_i}{\partial\ln T}-\frac{7}{3}\left(\frac{\partial\ln T}{\partial r}\right)^{-1}\frac{\cos\theta}{(R+r\cos\theta)}\right] \tag{42}$$

where κ_{er} , κ_{ir} denote the electron and ion thermal conductivities along the minor radius, respectively. Consequently, the total radial thermal conductivity is given by

$$\kappa_{r}=\frac{3n_i k_B}{4\mu_0\sigma_e(r)}\left[\frac{Z+2}{(Z+1)}+\frac{\partial\ln n_i}{\partial\ln T}-\frac{7}{3}\left(\frac{\partial\ln T}{\partial\ln r}\right)^{-1}\frac{r\cos\theta}{(R+r\cos\theta)}\right] \tag{43}$$

where κ_r represents the total radial thermal conductivity. The associated thermal diffusivities can be expressed as follows

$$\chi_{er}=\frac{\kappa_{er}}{n_e c_v}=\frac{1}{2(Z+1)\mu_0\sigma_e(r)}\left[1+\frac{\partial\ln n_i}{\partial\ln T}-\frac{7}{3}\left(\frac{\partial\ln T(\vec{r})}{\partial\ln r}\right)^{-1}\frac{r\cos\theta}{(R+r\cos\theta)}\right] \tag{44}$$

$$\chi_{ir}=\frac{\kappa_{ir}}{n_i c_v}=\frac{1}{2(Z+1)\mu_0\sigma_e(r)}\left[2+\frac{\partial\ln n_i}{\partial\ln T}-\frac{7}{3}\left(\frac{\partial\ln T(\vec{r})}{\partial\ln r}\right)^{-1}\frac{r\cos\theta}{(R+r\cos\theta)}\right] \tag{45}$$

They indicate that the electron radial thermal diffusivity is comparable in magnitude to that of the ions, in agreement with the experimental findings [4], [6], [26]. The radial thermal diffusivities are found to be inversely proportional to the electrical conductivity and decrease continuously toward the plasma core as the electrical conductivity increases, a trend consistent with the experimental results [4], [5], [6], [26], [28]. For the edge region of tokamak plasma with the previously adopted parameters, $\partial lnT/\partial lnn_i = 4$, $\partial lnn_i/\partial lnr = -10$, Z=1, T=10^6 K, a/R=1/3, the estimated thermal diffusivities are on the order of 1 m^2/s, which agrees with the

experimental results [4]–[8], [26], [35], [36], [37].

Using the same approach, the radial thermal conductivity based on the classical theory can be expressed as

$$\kappa_{rc}=\frac{5n_ik_B}{2}\frac{(Z+1)p_i}{\sigma_eB_\varphi^2}\left[\frac{Z+2}{(Z+1)}+\frac{\partial\ln n_i}{\partial\ln T}-\frac{7}{3}\left(\frac{\partial\ln T}{\partial\ln r}\right)^{-1}\frac{r\cos\theta}{(R+r\cos\theta)}\right]$$

where κ_{rc} denotes the classical radial thermal conductivity. The ratio of the radial thermal conductivity obtained in the work to its classical counterpart is given by

$$\frac{\kappa_r}{\kappa_{rc}}=\frac{3}{5(Z+1)}\frac{B_\varphi^2}{2\mu_0p_i} \tag{46}$$

This ratio indicates that the radial thermal conductivity derived here is several orders of magnitude higher than that predicted by the classical theory.

3.2.3 Density limit

As indicated previously, the diffusion of the tokamak plasma is sensitively dependent on the plasma temperature. The time-dependent temperature can be determined by adding the thermal transport equations for the electrons and ions [38] in thermal equilibrium

$$\frac{3}{2}k_B\frac{\partial(n_i+n_e)T}{\partial t}=\frac{\partial}{r\partial r}\left(\kappa r\frac{\partial}{\partial r}T\right)+(1-\gamma)p_{in}+p_{OHp}+p_{OHt}-p_{rad} \tag{47}$$

where p_{in} denotes the input power density, γ represents the fraction of the input power density that drives the electric current, p_{OHp} and p_{OHt} are the Ohmic heating power densities arising from the poloidal and toroidal currents, respectively, and p_{rad} is the radiation power density. Using the previously derived mean radial velocity and toroidal magnetic field, i.e., Eq. (12) and Eq. (16), the poloidal Ohmic heating power density p_{OHp} can be expressed as

$$p_{OHp} \approx \frac{B_\varphi^2(a)}{\mu_0^2 \sigma_e} \left\{ \frac{\partial}{\partial r} \left[\frac{p_i(a)}{p_i(r)} \right]^{\frac{3}{10(Z+1)}} \right\}^2 \tag{48}$$

The poloidal Ohmic heating is strongly dependent on both the toroidal magnetic field strength and the electrical conductivity. An increase in the toroidal magnetic field enhances the poloidal Ohmic heating power density and raises the plasma edge temperature, thereby improving the electrical conductivity and reducing the diffusion constant. The poloidal Ohmic heating increases gradually toward the plasma edge, reaching magnitudes on the order of 10^6 -10^7 W/m^3 at the edge.

The toroidal Ohmic heating power density is given by $p_{OHt} = j_p^2/\sigma_e$, where j_p denotes the toroidal electric current density. In contrast to the poloidal Ohmic heating, the toroidal Ohmic heating increases toward the plasma core. The radiation power density p_{rad} is given by $p_{rad} = n_e n_i L_Z(T)$ [39], [40], where $L_Z(T)$ represents the radiation loss rate. The radiation power density depends strongly on the electron and ion density. An increase in the ion density significantly enhances the radiation power density, which in turn leads to a sharp drop in the plasma temperature and an increase in the dimensionless exponent α_T. The substantial temperature reduction results in a decrease in the electrical conductivity, thereby increasing the radial diffusion constant and ultimately causing disruption of the tokamak plasma discharge.

For the steady-state tokamak plasma core, the power loss due to the thermal conductivity and the power gain from the poloidal Ohmic heating can be neglected, yielding the relation $p_{rad} \approx p_{OHt} + (1-\gamma)p_{in}$. Substituting the expressions for the radiation power density p_{rad} and the toroidal Ohmic heating power density yields

$$n_i \approx \sqrt{\frac{j_p^2}{ZL_Z(T)\sigma_e} + \frac{(1-\gamma)p_{in}}{ZL_Z(T)}} \tag{49}$$

For most experimental tokamak plasma [41], [42], the toroidal Ohmic heating power density at the plasma core typically lies in the range 10^5-10^6 W/m^3, and the average input power density over the entire plasma falls within a similar range. The simulations indicate that the input power density, particularly from the neutral beam injection, is mainly deposited in the regions r/a >0.2, with significantly lower deposition for r/a <0.2 [43]. Consequently, the input power density in the plasma core r/a <0.2 is much smaller than the average input power density, and is also considerably lower than the toroidal Ohmic heating power density, leading to the relation

$$n_i \approx \frac{j_p}{\sqrt{ZL_Z(T)\sigma_e}} \tag{50}$$

This indicates that the ions density limit in the tokamak plasma core depends sensitively on the radiation power density, the electric conductivity and the toroidal electric current density. According to the Coulomb collision mechanism, the electric conductivity is independent of the electron number density. Therefore, the ion density limit is proportional to the toroidal electric current density, in agreement with the empirical Greenwald density limit [44], [45].

The net charge number of ions represents an interesting parameter. Increasing the net charge number Z enhances the radiation power density [46], but significantly reduces the electrical conductivity according to $\sigma_e \propto Z^{-1}$. As a result, the ion density limit exhibits a weak dependence on Z. Its magnitude can be estimated using the typical parameters of the tokamak plasma core. For the hydrogen plasma with the temperature

10 *KeV*, the radiation loss rate may be dominated by the Bremsstrahlung radiation and is on the order of 10^{-36} $W{\cdot}m^3$ at [40], [42], while the electric conductivity is approximately the order of 10^8 S/m at the relevant temperature. The resulting ion density limit at the plasma core is estimated to be $n_i \approx 10^{14} j_p$, consistent with the empirical Greenwald density limit [44], [45].

The situation differs for the stellarator where the toroidal Ohmic heating power density in the plasma core can be neglected owing to the negligible toroidal current. In this case, the ion density limit at the plasma core is given by

$$n_i \approx \frac{\sqrt{p_{in}}}{\sqrt{ZL_Z(T)}} \tag{51}$$

which agrees with the experimental scaling law for the stellarators [47].

Turning to the steady-state plasma edge, the estimated thermal loss density is on the order of 10^5 W/m^3, significantly smaller than the radiation power density. Moreover, the power gain from the input power density and the toroidal Ohmic heating is much smaller than the poloidal Ohmic heating power density, whose magnitude can reach the order of 10^7 W/m^3. Consequently, the temperature evolution at the plasma edge is governed primarily by the poloidal Ohmic heating power density p_{OHp} and the radiation power density p_{rad}, yielding the relation $p_{rad} \approx p_{OHp}$. Substituting the related expressions leads to the ion density limit at the plasma edge

$$n_i \approx \frac{B_\varphi(a)}{\mu_0\sqrt{ZL_Z(T)\sigma_e}} \frac{3}{10(Z+1)} \left| \frac{\partial}{\partial r} \ln p_i(r) \right| \tag{52}$$

This indicates that the density limit at the plasma edge is proportional to the magnetic field strength, a result consistent with the experimental observations in the helicon

plasmas [48].

Considering the density limits at the plasma core and the edge, the overall density limit is primarily governed by the radiation loss rate, in agreement with the theoretical analysis [49]. The radiation loss rate can be significantly enhanced by the introduction of the high-Z impurities into the plasma [50]. Therefore, careful control of the impurity content is essential to avoid the excessive radiation loss and the resultant radiation collapse.

Based on the preceding discussion, several key aspects are important for the steady-state operation of a tokamak plasma. First, a sufficiently high electrical conductivity must be sustained by maintaining a high plasma temperature and a low density of the high-Z impurities. As the nuclear fusion intensifies, the resulting temperature rise further improves the confinement performance. Second, the radiation loss rate should be carefully minimized by controlling the impurity density and the temperature. Third, in addition to the toroidal bootstrap current, an additional electrical current is required at the plasma core for the long-pulse operation. Fourth, increasing the toroidal magnetic field enhances the plasma confinement by raising the edge temperature through the poloidal Ohmic heating.

3.3 Model assumptions and limitations

The analytical model developed above is built on several physical assumptions. Clarifying these assumptions and their associated limitations is essential for appropriate application of the model.

First, the semi-free electron picture relies on the condition that local charge neutrality

holds on timescales longer than the electric relaxation time (τ=$\varepsilon_0\varepsilon/\sigma_e$). This condition may be well satisfied in tokamak and inertial confinement fusion plasmas but may break down for the thermal-field emission electrons, or on timescales comparable to or shorter than the electric relaxation time.

Second, the derivation assumes that small-angle Coulomb collisions dominate the relaxation processes, thereby justifying the use of electron and ion relaxation times.

Third, the linearization $f_A = f_A^0 + f_A^1$ is justified only when the anisotropic perturbation remains small $f_A^1/f_A^0 \ll 1$. From the derived expressions, the validity conditions can be explicitly written as $f_A^1/f_A^0 \sim u_r/\sqrt{k_B T/m_e}$, a condition generally satisfied in tokamak plasmas.

Fourth, the present model describes transport on a collisional, diffusive baseline. It does not explicitly incorporate fluctuations or turbulence-induced anomalies.

Fifth, the derivation of the magnetic moment force assumes $|r_{Ac}\nabla B_z| \ll B_z$. Substituting the derived equations yields $\sqrt{m_e k_B T}\nabla ln p_i(r)/(Z+1)eB_\varphi \ll 1$, which is generally satisfied in tokamak plasmas.

Based on these assumptions, the model is valid for quasi−neutral, collision−dominated plasmas with moderate temperature and density gradients, small distribution anisotropy, and without overwhelming turbulence. Its predictive power is highest in standard tokamak plasmas. It might be least reliable (or inapplicable) in regions near magnetic field singularities, or under conditions where any of the above assumptions break down.

4. Comparison with the mainstream turbulence theory

The present work offers an alternative framework for understanding anomalous transport. Rather than attributing it primarily to turbulence, we revisit a collision-dominated description with two modifications: replacing the instantaneous Lorentz force by the magnetic moment force, and treating electrons as "semi-free" under quasi-neutral conditions.

4.1 Key differences

Table 1 summarizes the quantitative differences among classical, neoclassical, turbulence, and the present model. Several points merit emphasis.

Table 1. Comparison of key transport properties among classical, neoclassical, and the present model. $q_s=aB_\varphi/RB_\theta$ is safety factor [2], where a, R denote the minor radius and major radius, respectively, B_φ, B_θ represent the toroidal and poloidal magnetic field.

Feature	Classical theory	Neoclassical theory	Present model	Experimental evidence
Radial particle diffusivity D_r (m^2/s)	$\sim10^{-4}$	$\sim10^{-2}$	~1-10	~1-10
Radial thermal diffusivity χ_i, χ_e (m^2/s)	$\sim10^{-4}$	$\sim10^{-2}$	~1	~1
Field scaling $D_r \propto B_\varphi^\delta$	$\delta=-2$	$\delta=-2$ (with q_s^2 factor)	$\delta=0$ (no explicit B_φ de pendence)	Weak B_φ dependence [31]
Temperature scaling $D_r \propto T^\eta$	$\eta=-1/2$	$\eta=-1/2$	$\eta=3/2$	Confinement time $\tau \propto T^{3/2}$ [29,30]
Radial electric field E_r	Positive (outward)	Negative (inward)	Negative (inward)	Negative, $\sim10^4$ V/m [22], [33], [34]

Edge/internal transport barriers (ETB/ITB)	Not captured	Not captured	Explained via pressure profile	Observed in H-mode [21,22]
Greenwald density limit $n_i \propto j_p$	Not captured	Not captured	Derived from thermal balance $n_i \propto j_p$	Empirical scaling [43,44]

Footnotes for Table 1:

[a] Classical and neoclassical predictions adopt the uniform or toroidal magnetic field assumptions without the magnetic moment force or semi-free electron picture.

[b] Experimental ranges are representative values from tokamak edge plasmas ($T \sim 10^6$ K); detailed parameters vary with device and operating regime.

[c] The weak experimental dependence of D_r on B_φ is inferred from confinement time scaling $\tau \propto B_T^{0.15} I_P^{0.93}$ [31].

[d] Gyrokinetic turbulence models reproduce fluctuation spectra and critical gradients [50–54] but do not yield closed analytical expressions for transport coefficients. The present model is complementary in providing a collisional baseline.

First, gyrokinetic turbulence models, despite their success in reproducing fluctuation spectra and critical gradient thresholds [51, 52] have not yielded a closed-form analytical expression for transport coefficients. Instead, they rely on computationally intensive numerical simulations [53–55] and, in many cases, empirical adjustments to match experimental transport levels. In contrast, the present model provides explicit, parameter-free expressions for D_r χ, E_r, and the density limit directly from first principles.

Second, turbulence theory explains ETB and ITB primarily through shear suppression of turbulence [52]. The present model attributes barrier formation to modifications of temperature and pressure profiles that reduce the radial velocity.

Third, the two approaches address different aspects of the same observations. Turbulence explains fluctuations, critical gradients, and deviations from diffusive scaling. Consistent with theoretical analyses based on experimental results [15], the

present model provides a collisional baseline that already matches the magnitude and parametric trends of anomalous transport. They might be complementary rather than contradictory.

4.2 Precedence of the magnetic moment force

The concept of magnetic-moment-based confinement has precedent in magnetic mirror devices where invariance of the magnetic moment underlies particle reflection [10]. However, to our knowledge, this work is the first to show that the Lorentz force in tokamak plasmas, when gyro-averaged, reduces identically to the magnetic moment force. Together with the semi-free electron picture, this reformulation yields a closed analytical theory for anomalous transport.

5. Conclusion

In this work, we have developed a unified analytical theory for anomalous transport in tokamak plasmas based on two fundamental physical insights that challenge conventional descriptions.

First, the Lorentz force, when averaged over a complete gyroperiod, manifests as the magnetic moment force. This reformulation reveals that confinement in magnetized plasmas is governed by the magnetic moment force rather than the instantaneous Lorentz force. Second, free electrons in a quasi-neutral plasma should be regarded as "semi-free": their spatial degrees of freedom are constrained by the ions due to charge neutrality and the strong electrostatic force. Consequently, the electron distribution function depends on the spatial coordinates of the ions, fundamentally altering the treatment of electron transport.

Based on these premises, we construct a simple yet comprehensive analytical model that yields closed-form expressions for radial particle diffusion coefficients and thermal diffusivities. The model reproduces experimentally observed magnitudes, several orders higher than classical and neoclassical predictions without adjustable parameters or turbulence assumptions. It provides a unified explanation for the formation of ETB and ITB, linking them directly to modifications in temperature and pressure profiles. The derived radial electric field exhibits a negative sign and the correct order of magnitude, consistent with experimental measurements, a feature not captured by classical treatments. Furthermore, the model yields density limit scaling that agrees with the empirical Greenwald limit and its extensions.

These findings carry three important implications for fusion research. Theoretically, anomalous transport may be understood within a collision-dominated framework; the conventional Fokker–Planck equation should be modified to incorporate the magnetic moment force and the semi-free electron description. Experimentally, the model provides predictive scaling relations for confinement time and its weak dependence on magnetic field, consistent with multi-machine databases, while the derived expressions for radial electric field and its shear offer a basis for interpreting transport barrier dynamics. Operationally, steady-state reactor operation requires maintaining high electrical conductivity (through high temperature and low high-Z impurity content), controlling radiation losses, and sustaining auxiliary current drive at the plasma core; the poloidal Ohmic heating mechanism identified here

suggests that increasing the toroidal field can improve edge confinement by elevating edge temperature.

In summary, this work offers a potential resolution to a long-standing puzzle in plasma physics by demonstrating that anomalous transport in tokamak plasma does not require new physics beyond collisional transport, but instead arises from previously overlooked consequences of charge neutrality and orbit-averaged dynamics. Nevertheless, the model is limited to collision-dominated regimes and may require extension for near-collisionless plasmas or regions with strong magnetic field gradients. The revealed physical insights and the resulting analytical framework provide a new foundation for understanding confinement degradation and optimizing performance in future fusion reactors such as ITER and CFETR.

References

[1] A. A. Galeev, R. Z. Sagdeev, Transport phenomena in a collisionless plasma in a toroidal magnetic system, Sov. Phys. JETP **26** (1968) 233-240.

[2] F. L. Hinton, R. D. Hazeltine, Theory of plasma transport in toroidal confinement systems, Rev. Mod. Phys. **48** (1976) 239-308.

[3] S. X. Wang, H. Q. Liu, Y. X. Jie, W. X. Ding, L. Zeng, Y. W. Sun, H. Lian, X. Zhu, Z. Y. Zou, B. Lyu, Y. Y. Li, Q. Zang, H. F. Du, C. Zhou, A. D. Liu, T. Zhang, W. Gao, X. Gao and The EAST Team, Investigation of RMP induced density pump-out on EAST, Nucl. Fusion **58** (2018) 112013 (7pp).

[4] Y. Q. Chu, The transport characteristics of ITB on EAST, A dissertation for doctor's degree, University of Science and Technology of China, 2021, pp.66.

[5] P. C. Efthimion, L. C. Johnson, J. D. Strachan, E. J. Synakowski, M. Zarnstorff, H. Adler, C. Barnes, R. V. Budny, F. C. Jobes, M. Louglin, D. McCune, D. Mueller, A. T. Ramsey, G. Rewoldt, A. L. Roquemore, W. M. Tang, G. Taylor, Tritium particle transport experiments on TFTR during D-T operation, Phys. Rev. Lett. **75** (1995) 85-88.

[6] S. D. Scott, P. H. Dimond, R. J. Fonck, R. J. Goldston, R. B. Howell, K. P. Jaehnig, G. Schilling, E. J. Synakowski, M.C. Zarnstorff, C. E. Bush, E. Fredrickson, K. W. Hill, A. C. Janos, D. K. Mansfield, D. K. Owens, H. Park, G. Pautasso, A. T. Ramsey, J. Schivell, G. D. Tait, W. M. Tang, G. Taylor, Local measurement of correlated momentum and heat transport in the TFTR tokamak, Phys. Rev. Lett. **64** (1990) 531-534.

[7] A. J. Wootton, B. A. Carreras, H. Matsumoto, K. McGuire, W. A. Peebles et al. Fluctuations and anomalous transport in tokamaks, Phys. Fluids B **2** (1990) 2879.

[8] S. K. Kim, D. L. Brower, W. A. Peebles, N. C. Luhmann, JR. Experimental Measurement of Electron Particle Diffusion from Sawtooth-Induced Density-Pulse Propagation in the Texas Experimental Tokamak, Phys. Rev. Lett. **60** (1988) 577-580.

[9] V. A. Krupin, M. R. Nurgaliev, A. R. Nemets, I. A. Zemtsov, S. D. Suntsov, T. B. Myalton, D. S. Sergeev, N. A. Solovev, D. V. Sarychev, D. V. Ryjaov, S. N. Tugarinov, N. N. Naumenko, Ion heat transport in electron cyclotron resonance heated L-mode plasma on the T-10 tokamak Plasma Sci. Technol. **26** (2024) 045101 (9pp).

[10] J. L. Xu, S. X. Jin, Plasma Physics, Atomic energy press, Beijing, 1981.

[11] R. Balesc, Aspects of anomalous transport in plasmas, IOP Publishing Ltd. 2005, Institute of Physics Publishing, Bristol, UK, pp.1-5

[12] M. Ariola, A. Pironti, Magnetic control of tokamak plasma, 2nd edition, 2016, Springer International Publishing Switzerland, pp.25-28.

[13] M. Kikuchi, M. Azumi, Steady-state tokamak research: Core physics, Rev. Mod. Phys. **84** (2012)1807-1854.

[14] J. W. Connor, H. P. Wilson, Survey of theories of anomalous transport, Plasma Phys. Control. Fusion **36** (1994) 719-795.

[15] F. A. Haas, A. Thyagaraja, Conceptual and experimental bases of theories of anomalous transport in Tokamaks, Phys. Reports **143** (1986)240-276.

[16] J. Ongena, R. Koch, R.Wolf, H. Zohm, Magnetic-confinement fusion, Nat. Phys. **12** (2016) 398-410.

[17] A. Fasoli, S. Brunner,W. A. Cooper, J. P. Graves, P. Ricci, O. Sauter, L. Villard, Computational challenges in magnetic-confinement fusion physics, Nat. Phys. **12** (2016) 411-423.

[18] Y. J. Huang, Analytical Model for the Thermal Conductivity of Fully Ionized Plasmas, viXra: 2503.0090.

[19] S. Eliezer, The Interaction of High-Power Lasers with Plasmas, 2002, Institute of Physics Publishing, London, UK, pp.17-21, pp58-60, pp.183-198.

[20] B. A. Carreras, V. E. Lynch, G. M. Zaslavsky, Anomalous diffusion and exit time distribution of particle tracers in plasma turbulence model, Phys. Plasmas **8** (2001) 5096-5103.

[21] F. Albajar, J. Johner, G. Granata, Improved calculation of synchrotron radiation losses in realistic tokamak plasmas, Nucl. Fusion **41** (2001) 665.

[22] F Wagner, A quarter-century of H-mode studies, Plasma Phys. Control. Fusion **49** (2007) B1–B33.

[23] D. G. Whyte, A.E. Hubbard, J.W. Hughes, B. Lipschultz, J.E. Rice, E.S. Marmar, M. Greenwald, I. Cziegler, A. Dominguez, T. Golfinopoulos, N. Howard, L. Lin, R.M. McDermott, M. Porkolab, M.L. Reinke, J. Terry, N. Tsujii,

S.Wolfe, S.Wukitch, Y. Lin and the Alcator C-Mod Team, I-mode: an H-mode energy confinement regime with L-mode particle transport in Alcator C-Mod, Nucl. Fusion **50** (2010) 105005 (11pp).

[24] J. Chung, H. S. Kim, Y. M. Jeon, J. Kim, M. J. Choi , J. Ko, K. D. Lee, H. H. Lee, S. Yi, J. M. Kwon, S.-H. Hahn, W.H. Ko, J. H. Lee, S.W. Yoon, Formation of the internal transport barrier in KSTAR, Nucl. Fusion **58** (2018) 016019 (1-7pp).

[25] G. T. Hoang, C. Bourdelle, X. Garbet, G. Antar, R.V. Budny, T. Aniel, V. Basiuk, A. Bécoulet, P. Devynck, J. Lasalle, G. Martin, F. Saint-Laurent, and the Tore Supra Team, Internal Transport Barrier with Ion-Cyclotron-Resonance Minority Heating on Tore Supra, Phys. Rev. Lett. **84** (2000) 4593-4596.

[26] K. H. Burrell, S. L. Allen, G. Bramson, N. H. Brooks, R. W. Callis, T. N. Carlstrom, et al. Confinement physics of H-mode discharges in DIII-D, Plasma Phys. Control. Fusion **31** (1989) 1649-1664.

[27] E. M. Hollmann, F. Anderegg, C. F. Driscoll, Measurement of Cross-Magnetic-Field Heat Transport in a Pure Ion Plasma, Phys. Rev. Lett. **82** (1999) 4839-4842.

[28] R. J. Hawryluk, Results from deuterium-tritium tokamak confinement experiments, Rev. of Mod. Phys. **70**(1998) 537-587.

[29] R. Guirlet, C. Giroud, T. Parisot, M. E. Puiatti, C. Bourdelle, L. Carraro, N. Dubuit, X Garbet, P. R. Thomas, Parametric dependences of impurity transport in tokamaks, Plasma Phys. Control. Fusion **48**(2006) B63–B74.

[30] B. A. Carreras, Progress in Anomalous Transport Research in Toroidal Magnetic Confinement Devices, IEEE Trans. Plasma Sci., **25** (1997)1281-1321.

[31] L. A. Artsimovich, G. A. Bobrovsky, E. P. Gorbunov, D. P. Ivanov, V. D. Kirillov, E. I. Kuznetsov, S. V. Mirnov, M. P. Petrov, K. A. Razumova, V. S. Strelkov, D. A. Shcheglov, Experiments in tokamak devices, Nucl. Fusion **17** (1969) 17–24.

[32] ITER Physics Expert Group on Confinement and Transport, ITER Physics Expert Group on Confinement Modelling and Database, ITER Physics Basis Editors 1999 Nucl. Fusion 39, 2175.

[33] J Baldzuhn, M Kick, H Maassberg and the W7-AS Team, Measurement and calculation of the radial electric field in the stellarator W7-AS, Plasma Phys. Control. Fusion **40** (1998) 967–986.

[34] J. Schirmer, G. D. Conway, H. Zohm, W. Suttrop, ASDEX Upgrade Team, The radial electric field and its associated shear in the ASDEX Upgrade tokamak, Nucl. Fusion **46** (2006)S780-S791

[35] F. Kin, K. Itoh, T. Bando , K. Shinohara, N. Oyama, M. Yoshida , K. Kamiya, S. Sumida, Experimental evaluation of avalanche type of electron heat transport in magnetic confinement plasmas, Nucl. Fusion **63** (2023) 016015 (13pp).

[36] X. Garbet, P. Mantica, C. Angioni, E. Asp, Y. Baranov, C. Bourdelle, R. Budny, F. Crisanti, G. Cordey, L. Garzotti, N. Kirneva, D. Hogeweij, T. Hoang, F. Imbeaux, E. Joffrin, X. Litaudon, A. Manini, D. C. McDonald, H. Nordman, V. Parail, A. Peeters, F. Ryter, C. Sozzi, M. Valovic, T. Tala1, A. Thyagaraja, I.

Voitsekhovitch, J. Weiland, H. Weisen, A. Zabolotsky and the JET EFDA Contributors, Physics of transport in tokamaks, Plasma Phys. Control. Fusion **46** (2004) B557–B574.

[37] C. E. Bush, S. A. Sabbagh, S. J. Zweben, R. E. Bell, E. J. Synakowski, G. Taylor, S. Batha, M. Bell, M. Bitter, N. L. Bretz, R. Budny, Z. Chang, D. S. Darrow, P. C. Efthimion, D. Ernst, E. Fredrickson, G. R. Hanson, L. C. Johnson, J. Kesner, B. LeBlanc, F. M. Levinton, D. Mansfield, M. E. Mauel, E. Mazzucato, D. McCune, M. Murakami, R. Nazikian, G. A. Navratil, H. Park, S. F. Paul, C. K. Phillips, M. H. Redi, J. Schivell, S. D. Scott, C. H. Skinner, H. H. Towner, J. B. Wilgen, M. C. Zarnstorff, and the TFTR Group, Deuterium–tritium high confinement (H-mode) studies in the Tokamak Fusion Test Reactor, Phys. Plasmas **2** (1995) 2366.

[38] J. Hugill, Transport in Tokamak-A Review of Experiment, Nucl. Fusion **23** (1983) 331-373.

[39] D. K. Morozov, E. O. Baronova, I. Yu. Senichenkov, Impurity Radiation from a Tokamak Plasma, Plasma Phys. Rep. **33**, 2007, pp. 906–922.

[40] C. Breton, C. De Michelis, M. Mattioli, Radiation losses from oxygen and iron impurities in a high-temperature plasma, Nucl. Fusion **16** (1976)891-899.

[41] J. Wesson, Tokamaks. 4th Edition, 2011, Oxford Science Publications, International Series of Monographs on Physics, Volume 149.

[42] K. Miyamoto, Plasma Physics for Controlled Fusion, second edition, 2016, Spring-Verlag Berlin Heidelberg, pp.340, pp.351, pp.376

[43] M. Schneider, L.-G. Eriksson, I. Jenkins, J.F. Artaud, V. Basiuk, F. Imbeaux, T. Oikawa, ITM-TF contributors and JET-EFDA contributors, Simulation of the Neutral Beam Deposition within Integrated Tokamak Modelling Frameworks, Nucl. Fusion **51** (2011) 063019.

[44] M. Greenwald, J. L. Terry, S. M. wolfe, S. Ejima, M.G. Bell, S.M. Kaye, G. H. Neilson, A new look at density limits in tokamaks, Nucl. Fusion **28** (1988) 2199-2207.

[45] Martin Greenwald, Density limits in toroidal plasmas, Plasma Phys. Control. Fusion **44** (2002)R27-R80.

[46] R. V. Jensen, D. E. Post, W. H. Grasberger, C. B. Tarter, W. A. Lokke, Calculations of impurity radiation and its effects on tokamak experiments, Nucl. Fusion **17** (1977)1187-1196.

[47] S. Sudo, Y. Takeiri, H. Zushi, F. Sano, K. Itoh, K. Kondo, A. IIyoshi, Scalings of energy confinement and density limit in stellarator/heliotron devices, Nucl. Fusion **30** (1990)11-21.

[48] J.G. Kwak, S.K. Kim, Suwon Cho, Upper limit to the monotonic increasing dependence of the plasma density on the magnetic field in helicon discharges, Phys. Lett. A **267** (2000) 384–388.

[49] D. A. Gates, L. Delgado-Aparicio, Origin of Tokamak Density Limit Scalings, Phys. Rev. Lett. **108** (2012) 165004.

[50] R.V. Jensen, D. E. Post, W. H. Grasberger, C. B. Tarter, W. A. Lokke, Calculations of impurity radiation and its effects on tokamak experiments, Nucl. Fusion **17** (1977) 1187.

[51] W. L. Zhong, K. J. Zhao,X. L. Zou, J. Q. Dong, Recent progress on turbulence and multi‐scale interactions in tokamak plasmas, Rev. Mod. Plasma Phys. **4:11** (2020) 1-29.

[52] A Diallo, F M Laggner, Review: Turbulence dynamics during the pedestal evolution between edge localized modes in magnetic fusion devices, Plasma Phys. Control. Fusion **63** (2021) 013001 (1-19)

[53] K. Höfler , T. Görler, T. Happel, C. Lechte, P. Molina, M. Bergmann, R. Bielajew, G. D. Conway, P. David, S. S. Denk, R. Fischer, P. Hennequin, F. Jenko, R.M. McDermott, A. E. White, U. Stroth, & the ASDEX Upgrade Team, Milestone in predicting core plasma turbulence: successful multi-channel validation of the gyrokinetic code GENE, Nat. Commun. **16** (2025) 2558(1-11)

[54] G. Staebler, C. Bourdelle, J. Citrin, R. Waltz, Quasilinear theory and modelling of gyrokinetic turbulent transport in tokamaks, Nucl. Fusion **64** (2024) 103001 (60pp).

[55] Y. S. Na, T. S. Hahm, P. H. Diamond, A. D. Siena, J. Garcia, Z. Lin, How fast ions mitigate turbulence and enhance confinement in tokamak fusion plasmas, Nat. Rev. Phys. **7** (2025) 190 – 202.